COMPARISON OF SYSTEMS FOR LEVITATION HEATING OF ELECTRICALLY CONDUCTIVE BODIES

Ivo Doležel[1], Pavel Dvořák[2], Martin Mach[2], Bohuš Ulrych[2]
[1]*Faculty of Electrical Engineering CTU, Technická 2, 166 27 Praha 6, E-mail: dolezel@fel.cvut.cz*
[2]*Faculty of Electrical Engineering UWB, Sady Pětatřicátníků 14, 314 06, E-mail:{pdvorak,mach,ulrych}@kte.zcu.cz*

Summary Levitation heating of nonmagnetic electrically conductive bodies can be realized in various systems consisting of one or more inductors. The paper deals with comparison of the resultant Lorentz lift force acting on such a body (cylinder, sphere) and velocity of its heating for different shapes of coils and parameters of the field currents (amplitude, frequency). The task is solved in quasi-coupled formulation. Theoretical considerations are supplemented with an illustrative example whose results are discussed.

1. INTRODUCTION

Levitation heating of solid electrically conductive bodies is used in a number of various modern technologies. One of them is, for example, levitation melting of metals in an inert atmosphere.

Design and optimization of the device whose fundamental part is represented by one or several field coils in an appropriate arrangement and investigation of the complete process require, however, reliable mathematical and computer models providing complete information about its characteristics and overall efficiency.

The most important parameters playing the fundamental role in the process are the total repulsive electrodynamic force acting on the body and velocity of its heating. These quantities depend on particular disposition of the system and should be in such relations that the efficiency of the process is as high as possible.

Disposition of the field coils may differ from one case to another (their shapes can be cylindrical, conical or even more sophisticated). In specific applications the system may be placed in transversal magnetic field produced by supplementary coils that provides stabilizing rotation of the processed workpiece etc.

The paper represents only an introductory study whose aim it to obtain a sufficient amount of information about dimensioning of such a device from the viewpoint of the shape and other parameters of the field coil that would secure both the proposed position of the workpiece and its sufficiently fast heating. This task represents a coupled electromagnetic-temperature problem that is solved in a quasi-coupled formulation.

The subsequent task – computer modeling of melting of the levitated material and its behavior in applied electromagnetic field representing a coupled magnetohydrodynamic-temperature problem and associated solution of the free level of melt is now being prepared and is not included in this paper.

2. DESCRIPTION OF THE TECHNICAL PROBLEM

Consider an axi-symmetric levitating system consisting of one coil of a suitable shape (Fig. 1) in a cylindrical coordinate system r, z. The system consists of two active parts: an inductor **1** carrying harmonic current of amplitude I and frequency f and a well electrically conductive body **2** that is to be levitated and heated.

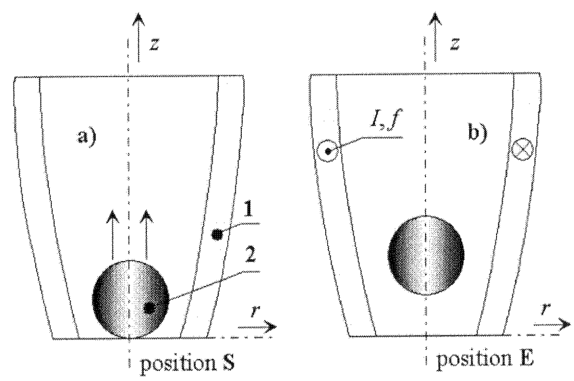

1- inductor, 2 - heated body

Fig. 1. The investigated arrangement.

At the time $t = 0$ the inductor **1** is connected to the source of harmonic current (I, f) and starts producing harmonic magnetic field. This field induces eddy currents $\boldsymbol{J}_{\mathrm{eddy}}$ in the body **2**. Interaction between the magnetic field and eddy currents induced in the body then produces the Lorentz forces that make it move up from the starting position **S** (Fig. 1a) in the direction of the indicated arrows. At the same time the body starts to be heated by the Joule losses. After a short transient taking time t_1 the body reaches the end position **E** where the Lorentz forces acting on it are in balance with its weight (Fig. 1b).

Growing temperature of the inductor and, particularly, processed body affects the physical properties of the system, among other electrical conductivity of its parts. Its variation influences distribution of magnetic field and, consequently, the position **E**. On the other hand, these variations are relatively small and in most cases may be neglected.

The final step is melting of the body and eventual shaping of the melt. We will model, however, the process, only to an time instant t_2 when the average temperature of the body reaches a prescribed value T_A while the maximum temperature T_M is still below the point of melting.

The aim of the paper is to test (the shape of the processed body being known in advance)

- various types of inductor **1** in order to find its optimized shape,
- parameters of the field current (I, f) that would ensure the most efficient regime of heating with respect to possible requirements (velocity, uniformity).

3. MATHEMATICAL MODEL AND ITS SOLUTION

Investigated were several typical examples that provided a lot of results. Due to rather limited space we shall focus, however, only on a conical inductor and spherical workpiece.

The mathematical model of the problem generally consists of two partial differential equations describing electromagnetic and temperature fields in the system and formulas for quantification of Lorentz' forces acting on the levitated sphere.

Harmonic magnetic field and associated quantities

Its definition area is depicted in Fig. 2. Line ABCD is the artificial boundary of the arrangement that represents the infinity (position of this boundary follows from several preliminary computations that show when the field distribution near the inductor **1** depends no longer on its distance). The investigated domain contains four subregions $\Omega_1, \ldots, \Omega_4$ with different physical parameters, the first two corresponding to the parts in Fig. 1.

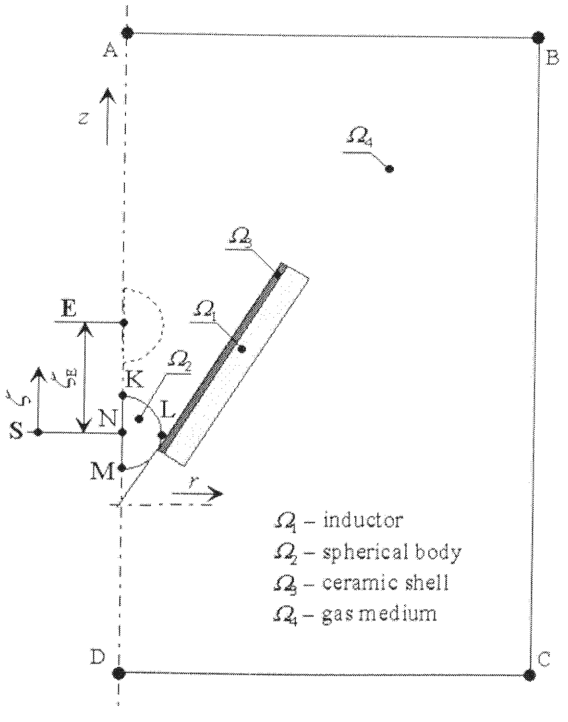

Fig. 2. Definition area of the problem.

As the system is linear, the electromagnetic field distribution may be described by Helmholtz' equation for the phasor of vector potential $\underline{\boldsymbol{A}}$. Because the field is considered axisymmetric (so that the vector potential as well as the densities of both field and eddy currents have only one nonzero component in tangential direction φ_0), this equation reads [1]

$$\frac{\partial^2 \underline{A}_\varphi}{\partial r^2} + \frac{1}{r}\frac{\partial \underline{A}_\varphi}{\partial r} - \frac{\underline{A}_\varphi}{r^2} + \frac{\partial^2 \underline{A}_\varphi}{\partial z^2} - \mathrm{j}\cdot\omega\gamma\mu_0 \underline{A}_\varphi = -\mu_0 \underline{J}_{\mathrm{ext}\varphi} \tag{1}$$

where γ denotes the electrical conductivity (which is generally a function of temperature T), $\mu_0 = 4\pi\cdot 10^{-7}$ H/m is the magnetic permeability of vacuum and ω is the angular frequency of the field current I. The phasor of their density is denoted as $\underline{J}_{\mathrm{ext}\varphi}$ and is supposed to be known (the current parameters are supposed to be constant in time).

The conditions along the boundary ABCDA read as follows:

- AD - antisymmetry, $\underline{A}_\varphi = 0$,
- ABCD - a force line along which $\underline{A}_\varphi = \mathrm{const}$. The condition of continuity of the vector potential implies that this constant is identically equal to zero.

The calculated distribution of the phasor of vector potential $\underline{A}_\varphi = \underline{A}_\varphi(r,z)$ then provides distribution of eddy currents $\underline{J}_{\mathrm{eddy}\varphi}$, specific Joule's losses w_J and average specific Lorentz' forces f_L acting on the heated sphere. These quantities are described by relations [2], [3]

$$\underline{J}_{\mathrm{eddy}\varphi} = -\mathrm{j}\cdot\omega\gamma\underline{A}_\varphi , \tag{2}$$

$$w_J = \frac{\underline{J}_{\mathrm{eddy}\varphi}\cdot\underline{J}^*_{\mathrm{eddy}\varphi}}{\gamma} \tag{3}$$

and

$$\boldsymbol{f}_L = \boldsymbol{J}_{\mathrm{eddy}} \times \boldsymbol{B} \ , \tag{4}$$

where $\underline{J}^*_{\mathrm{eddy}\varphi}$ is the complex conjugate to $\underline{J}_{\mathrm{eddy}\varphi}$. Now it is necessary to analyze the last expression for $\boldsymbol{f}_L$. It can easily be shown that this quantity can be expressed as

$$\boldsymbol{f}_L = \underline{\boldsymbol{J}}_{\mathrm{eddy}} \times \underline{\boldsymbol{B}}^* = \underline{\boldsymbol{J}}_{\mathrm{eddy}} \times \mathrm{rot}\,\underline{\boldsymbol{A}}^* = \mathbf{r}_0 f_{Lr} + \mathbf{z}_0 f_{Lz} = \mathbf{r}_0 \cdot \frac{\underline{J}_{\mathrm{eddy}\varphi}}{r}\cdot\frac{\partial}{\partial r}\left(r\underline{A}^*_\varphi\right) - \mathbf{z}_0\cdot\underline{J}_{\mathrm{eddy}\varphi}\cdot\frac{\partial \underline{A}^*_\varphi}{\partial z}. \tag{5}$$

Total Lorentz' force $\boldsymbol{F}_L$ acting on the sphere has only one component F_{Lz} in the axial direction that is given as

$$F_{Lz} = \int_{V_2} f_{Lz}\cdot \mathrm{d}V = -\int_{V_2} \underline{J}_{\mathrm{eddy}\varphi}\cdot\frac{\partial \underline{A}^*_\varphi}{\partial z}\cdot \mathrm{d}V , \tag{6}$$

where V_2 is the volume of the sphere.

Nonstationary temperature field

The nonstationary temperature field is calculated only in the heated sphere, i.e. in domain Ω_2 bounded by semicircle KLMNK. The basic Fourier-Kirchhoff equation generally describing its distribution reads [4]

$$\operatorname{div}(\lambda \cdot \operatorname{grad} T) = \rho c \cdot \left(\frac{\partial T}{\partial t} + \boldsymbol{v} \cdot \operatorname{grad} T \right) - w_\mathrm{J} \quad (7)$$

where λ denotes the thermal conductivity, ρ the specific mass of the heated material, c its specific heat and $\boldsymbol{v}$ its velocity. The term containing product $\boldsymbol{v} \cdot \operatorname{grad} T$ can be, however, omitted, because heating of the sphere is supposed in the stabilized position **E** (whose variations with changing temperature are neglected).

The boundary conditions are (see Fig. 2):

- KNM – symmetry: $\dfrac{\partial T}{\partial r} = 0$,
- KLM – convection: $-\lambda \cdot \dfrac{\partial T}{\partial z} = \alpha (T - T_\mathrm{ext})$

where α is the coefficient of the convective heat transfer and T_ext the known temperature of ambient medium.

4. ILLUSTRATIVE EXAMPLES

For the particular arrangement depicted in Figs. 1, 2 and 3 it is necessary to find

- Current of amplitude I and frequency f that would ensure
  - levitation of the processed sphere from the starting position **S** ($\varsigma_1 = \varsigma_\mathrm{S} = 0$), see Fig. 2, to final position **E** ($\varsigma_2 = \varsigma_\mathrm{E}$) where $F_{\mathrm{L}z} = F_\mathrm{g}$, F_g being the weight of the body,
  - its consequent induction heating to average temperature $T_\mathrm{A} = 650\,^\circ\mathrm{C}$,

Input data

The basic dimensions of the system (see Fig. 3) are:

- $R_0 = 0.05$ m, $h = 0.1$ m, $r_1 = 0.04$ m,
- $l = 0.178$ m, $s_1 = 0.003$ m, $s_2 = 0.002$ m,
- $\beta = 30$, 45 and 60°, respectively.

The coil is made from a hollow copper (Cu 99) conductor (internal diameter 4 mm, external diameter 8 mm) cooled by water. Its arrangement and dimensions are depicted in Fig. 3. The number of its turns that are wound in two layers $N_\mathrm{c} = 36$.

The principal physical parameters of Cu 99: electrical conductivity $\gamma_\mathrm{Cu} = 5.7 \cdot 10^7$ S/m, $\mu_\mathrm{r} = 1$.

Material of the sphere is aluminum Al 99.5 with the following properties: the temperature-dependent electrical conductivity γ_Al is in Fig. 4, $\mu_\mathrm{r} = 1$, $\lambda = 229$ W/mK, $\rho = 2700$ kg/m³, $c = 896$ J/kgK. Mass of the sphere $m = 1.45560$ kg and its weight $F_\mathrm{g} = 13.87$ N. The convective coefficient of heat transfer $\alpha = 20$ W/m²K and $T_\mathrm{ext} = 20$ °C. Magnetic permeability of electrically nonconductive ceramic shell **3** of the field coil is equal to μ_0.

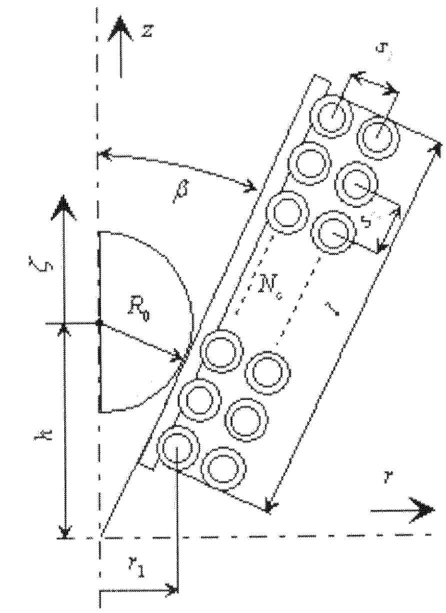

Fig. 3. The main details of the coil.

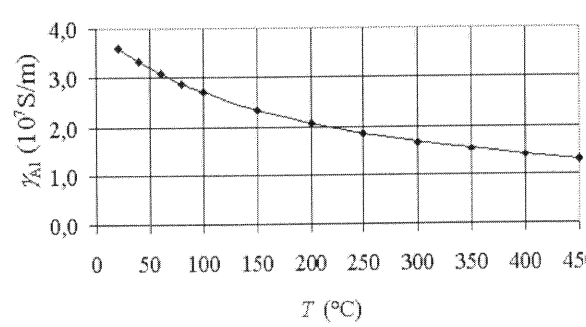

Fig. 4. Temperature dependence of electrical conductivity of used aluminum Al 99.5.

Selected results

Numerical solution of the problem was carried out by combination of professional FEM-based code supplemented with a number of single-purpose user programs written in Matlab and Borland Delphi.

First of all, investigated was the geometrical convergence of the results. Relevant computations checked the total magnetic energy in the domain with growing density of the discretization mesh. The values showing the geometrical convergence are given in Tab. 1.

As follows from the table, meshes with more than about 100000 elements provides sufficiently accurate (three valid digits) computation of magnetic field and consequent integral quantities such as energy, total Joule losses, total Lorentz force etc.

Therefore, all further computations were performed on a mesh with about 100000 nodes.

Tab. 1. Geometrical convergence of results.

Nodes	35572	81581	105357	259912
W_m (J)	67.98	67.61	68.47	68.47
F_{Lz} (N)	42.21	42.13	42.13	42.12

Note: the values in the table were calculated for parameters $I = 1760$ A, $f = 1$ kHz and $\beta = 30°$, $\varsigma = 0.011$ m.

For example, Fig. 5 contains a map of magnetic field for a triple of parameters I, f, β when the aluminum sphere reaches its end position **E**. Due to high electrical conductivity of the sphere eddy currents induced in it prevent magnetic field from penetrating into its deeper layers. That is why the eddy currents act only in its surface layers.

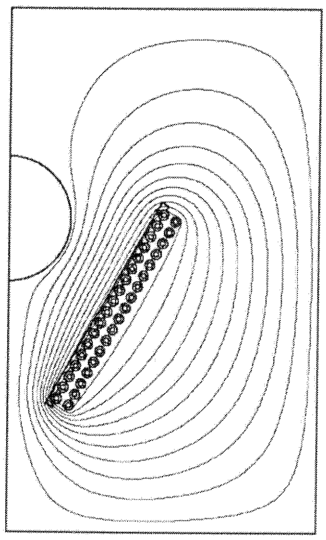

Fig. 5. Distribution of magnetic field in the system ($I = 1000\,A$, $f = 5\,kHz$, $\beta = 30°$).

Then we calculated the dependence of lift ς_E and specific average Joule losses w_J for current $I = 1000$ A and various angles β in order to find the most efficient arrangement. The results are depicted in Fig. 6.

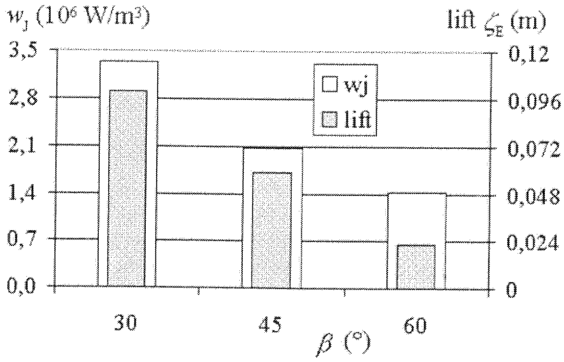

Fig. 6. Dependence of the specific Joule losses w_J and lift ς_E ($I = 1000\,A$, $f = 5\,kHz$) on angle β.

As could be expected, the highest values are reached in case of the field coil with conicity $\beta = 30°$, because its sides are relatively near the heated sphere. Therefore, all further calculations will be performed for this angle.

Next computations should evaluate the influence of frequency f of the field current. The results are depicted in Fig. 7.

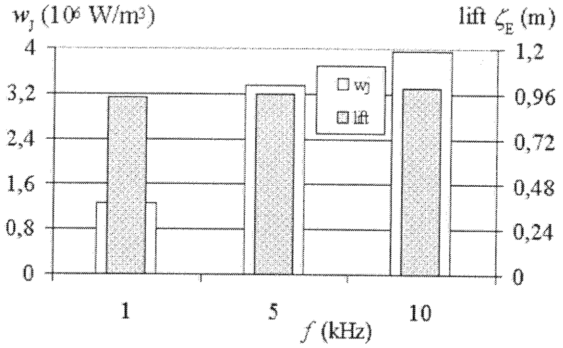

Fig. 7. Dependence of the specific Joule losses w_J and lift ς_E ($I = 1000\,A$, $\beta = 30°$) on frequency f.

As can be seen from this figure, even when the lift ς_E remains almost the same, the average Joule losses w_J strongly grows with increasing frequency. But as the design of a current source that would be able to provide such high parameters ($I = 1000$ A, $f = 10$ kHz) would be complicated and expensive, we accepted frequency $f = 5$ kHz.

Therefore, next calculations were performed for angle $\beta = 30°$ and frequency $f = 5$ kHz while current I varies within the range in which the temperature of the field winding does not exceed in time t_2 the maximal permissible temperature $T_A = 650$ °C.

The next step was calculation of the static characteristics of the system that describe the dependence of the total electromagnetic force F_{Lz} (6) on lift ς and value of the field current I for the selected parameters $f = 5$ kHz, $\beta = 30°$. The results are depicted in Fig. 8a.

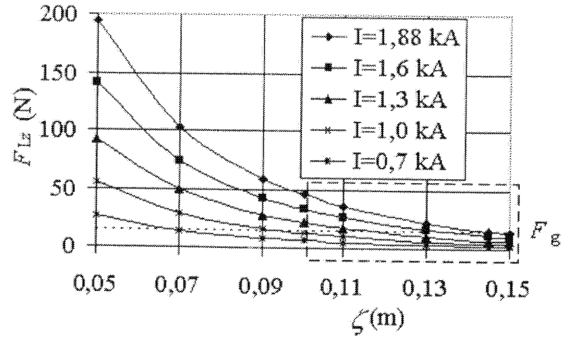

The figure also includes the straight line expressing weight F_g of the sphere. Its intersections with particular curves yield the dependence of the end position ς_E of the sphere on the field current I. In order to see better the shape of the static characteristics for higher values of ς and also the corresponding intersections, Fig. 8b contains a zoom of Fig. 8a bounded by the dotted rectangle.

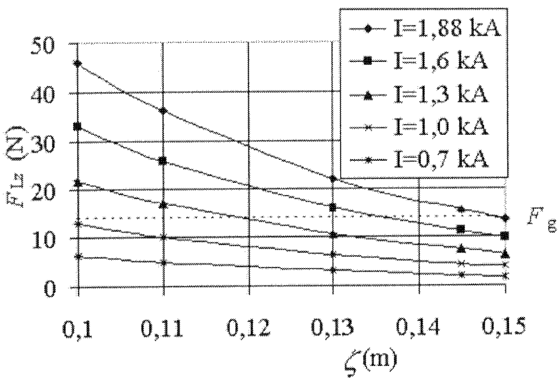

Fig.8b. Zoom of Fig. 8a.

Dependence of balanced position ς_E as a function of current I (derived from Figs. 8a and 8b) is depicted in Fig. 9.

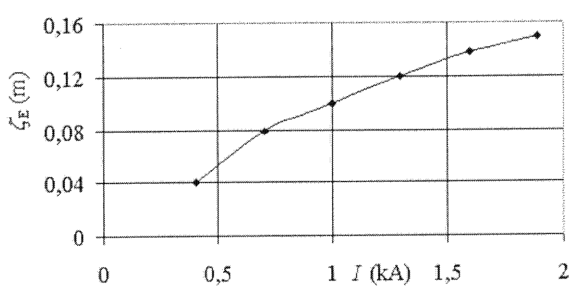

Fig. 9. Dependence of the end position ς_E on current I ($f = 5\,kHz$, $\beta = 30°$).

Of great importance are dependencies of the average Joule losses w_J and time t_2 of heating of the sphere (on the average temperature $T_A = 650\,°C$) on field current I. Both curves are depicted in Figs. 10 and 11.

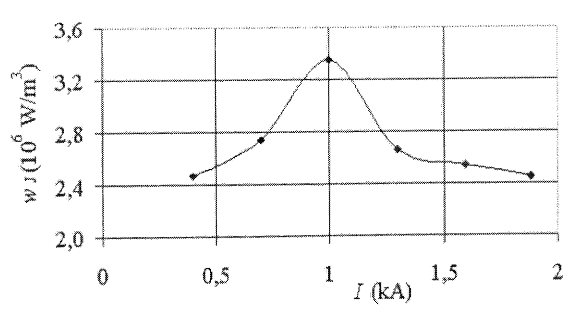

Fig. 10. Dependence of the average Joule losses w_J on field current I ($f = 5\,kHz$, $\beta = 30°$).

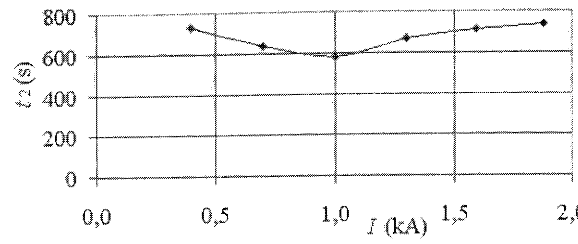

Fig. 11. Dependence of time t_2 on field current I ($f = 5\,kHz$, $\beta = 30°$).

The shape of both curves originates from the conicity of the field coil. For small currents I the end position ς_E is small and eddy currents (even when the sphere is still near the coil side) are also not high. With growing current I the end position ς_E is farther from the coil but eddy current still grow due to higher field current. So we found a maximum there. With ever growing current the lift is higher and higher, the distance between the sphere and coil also increases and the losses decrease.

An example of the obtained temperature field for time $t_2 = 580\,s$ and mentioned parameters I, f, β. It can be seen that the temperature is distributed fully uniformly overall the sphere, which is caused by its high thermal conductivity. Somewhat lower temperature along its surface is because of the heat convection into ambient medium.

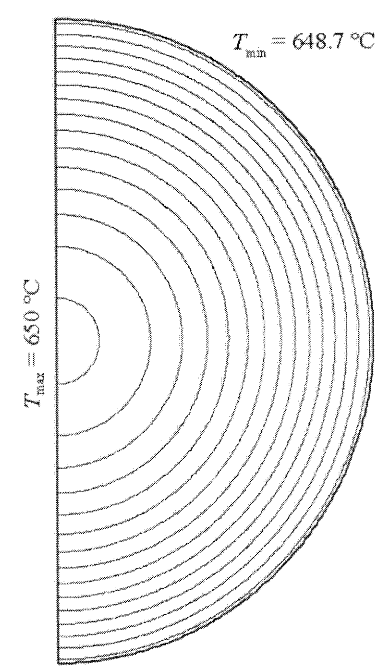

Fig. 12. Distribution of temperature field in the sphere ($I = 1000\,A$, $f = 5\,kHz$, $\beta = 30°$).

5. CONCLUSION

The results obtained may be summarized as follows:

- we found the optimal arrangement of the conical inductor in the given range providing the highest value of the Joule losses w_J : its conicity $\beta = 30°$ (see Fig. 6),
- we also found the optimal field current providing the highest velocity of heating on the prescribed temperature $T_A = 650\,°C$ (see Figs. 10 and 11),
- velocity of heating on the required temperature strongly depends on frequency of the field current (see Fig. 7),
- due to high thermal conductivity of aluminum, distribution of the temperature field is practically uniform, see Fig. 12 (this is usually desirable).
- Next work in the field will be aimed at the investigation of various other shapes of the inductor in order to accelerate the process and increase its efficiency.

Acknowledgment

This work has been financially supported from the Grant Agency of the Czech Republic (project No. 102/04/0095).

REFERENCES

[1] J. Stratton, "Electromagnetic theory", McGraw Hill Book, Co. NY, 1941.
[2] M.V.K. Chari, S.J. Salon, "Numerical methods in electromagnetism," Academic Press, 2000.
[3] N. Ida, "Engineering electromagnetics," Springer, 2000.
[4] J.P. Holman, "Heat transfer," McGraw Hill, 2002.
[5] www.quickfield.com.